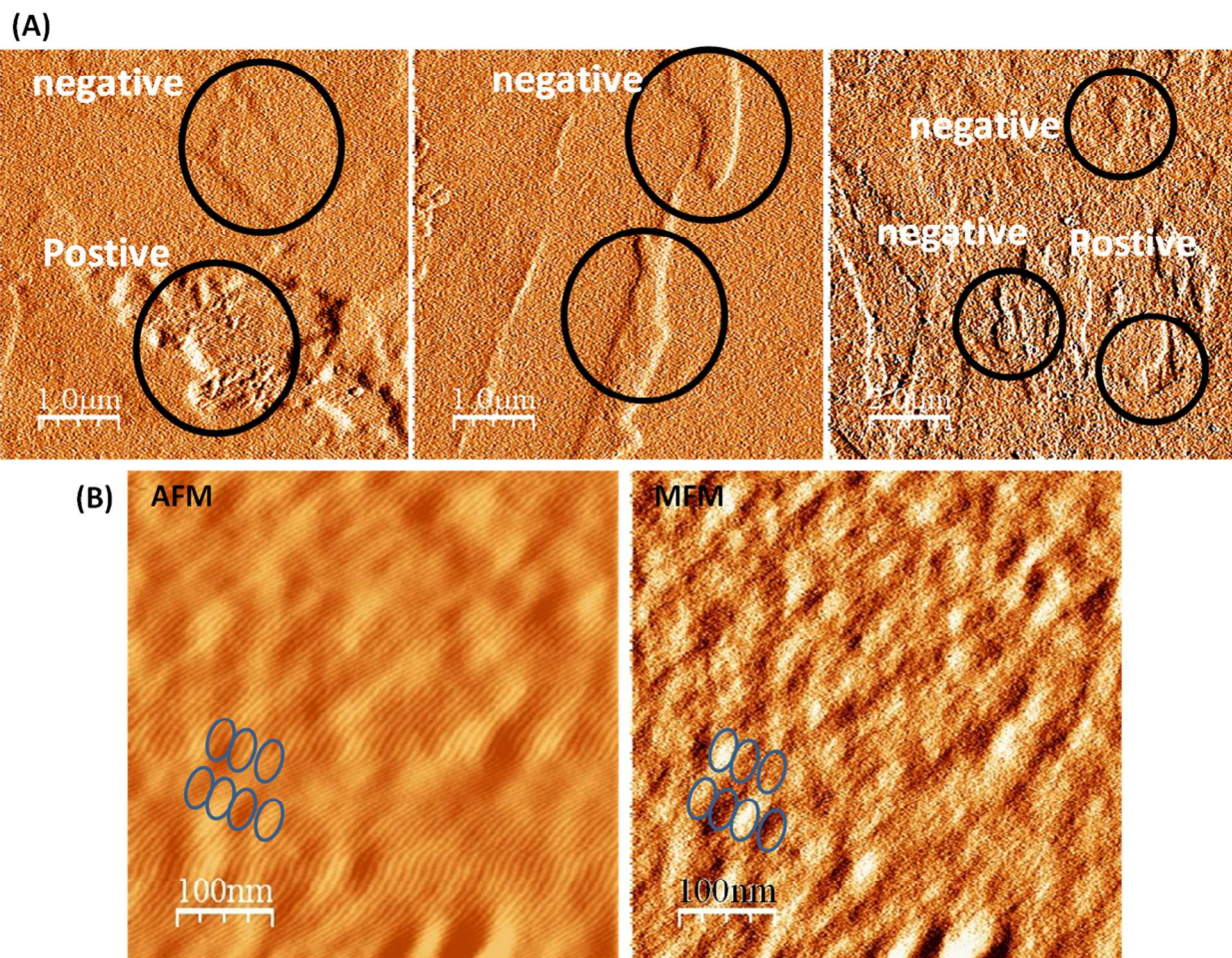


# Supporting Information - Chemically Engineered Graphene-Based 2D Organic Molecular Magnet

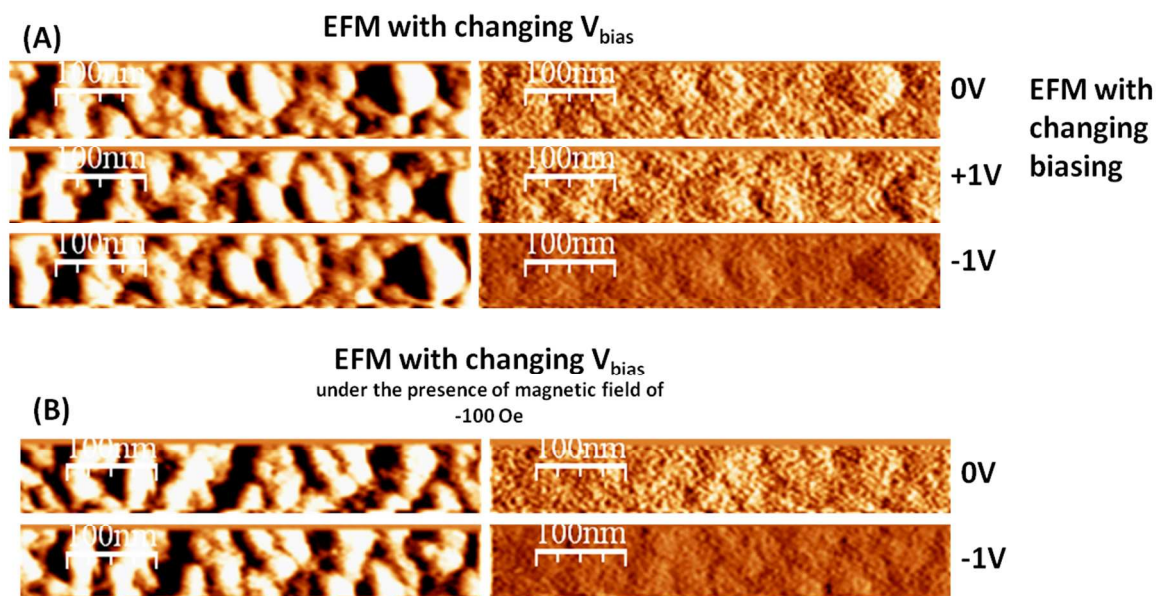
*Jeongmin Hong, Elena Bekyarova, Walt A. de Heer, Robert C. Haddon, and Sakhrat Khizroev*

**Table S1.** Exchange coupling field extracted from the MOKE experiments, a signature of antiferromagnetic coupling ( $H_{\text{bias}}$ ).

Region	$H_{\text{bias}}$ (Oe)
1	3305.129
2	3121.299
3	3191.634
4	3285.947
5	3621.637
6	3745.523
7	11,245.8
8	12,445.5
9	6553.333
10	2344.415

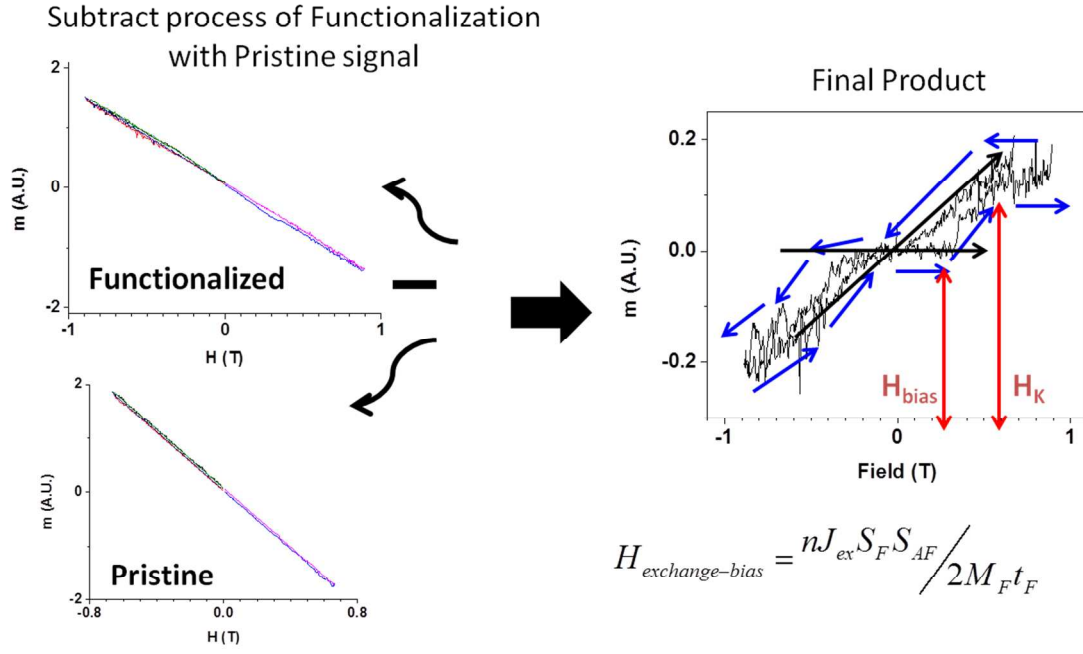


**Figure S1.** Macroscale MFM images of NP-EG structures. **(A)** The domain structures of magnetization pointing up and down in high-density functionalized graphene. **(B)** The mixed topology and magnetic phase of smaller domain structures of magnetization pointing up and down next to each other in functionalized graphene on a smaller scale.



**Figure S2.** EFM images of functionalized graphene structures obtained by changing the voltage bias (**A**) and the magnetic field (**B**) in the same region. This behavior allows for the possibility of controlling the magnetic phase through external parameters such as the voltage bias.

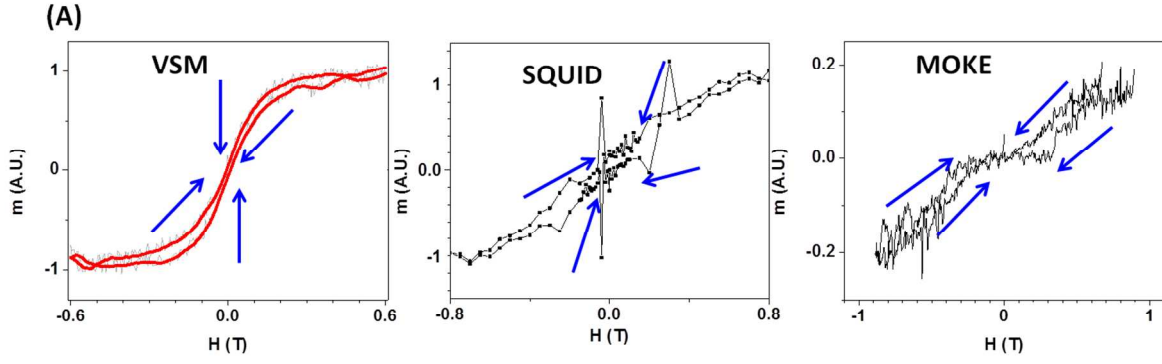
MOKE measurement in the Out-of-Plane component at Room-Temperature  
(Subtraction Process: the signal of NP-EG from pristine EG)



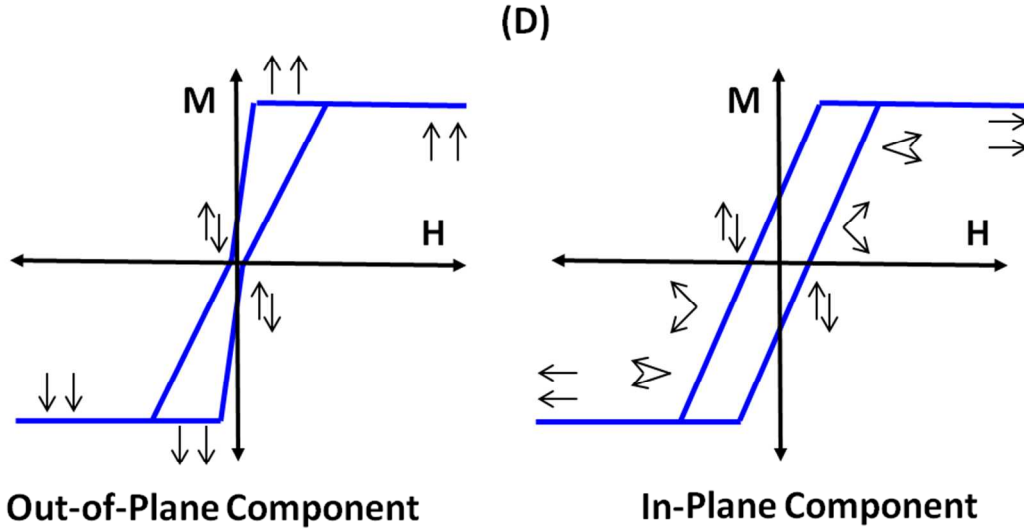
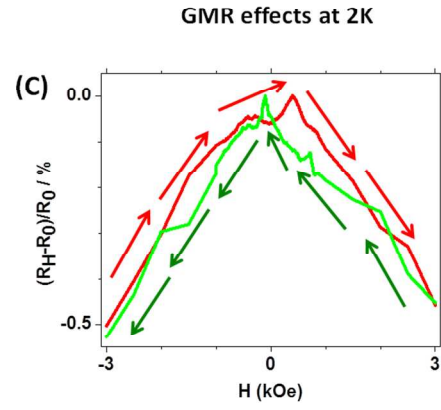
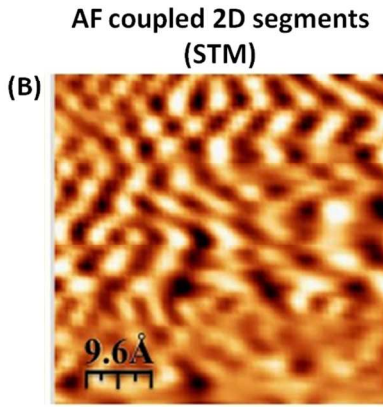
**Figure S3.** Subtraction of MOKE data before and after functionalization at room temperature.

Illustration of m-H loops from MOKE data such as exchange-bias and anisotropy fields.





**Comparison of Out-of-Plane Component Measurements:  
A signature of antiferromagnetically coupled regions**



**Figure S4.** (A) Comparison of out-of-plane measurement data from three different types of measurements: VSM, SQUID, and MOKE. (B) STM images of antiferromagnetically coupled segments. (C) GMR effects of functionalized graphene at 2 K in the out-of-plane component.

The graphene presenting the zero field resistance is significantly different from the parallel case indicating the presence of a GMR effect. (D) Possible scenario of an experimental model of m-H loops in the in-plane and out-of-plane components.

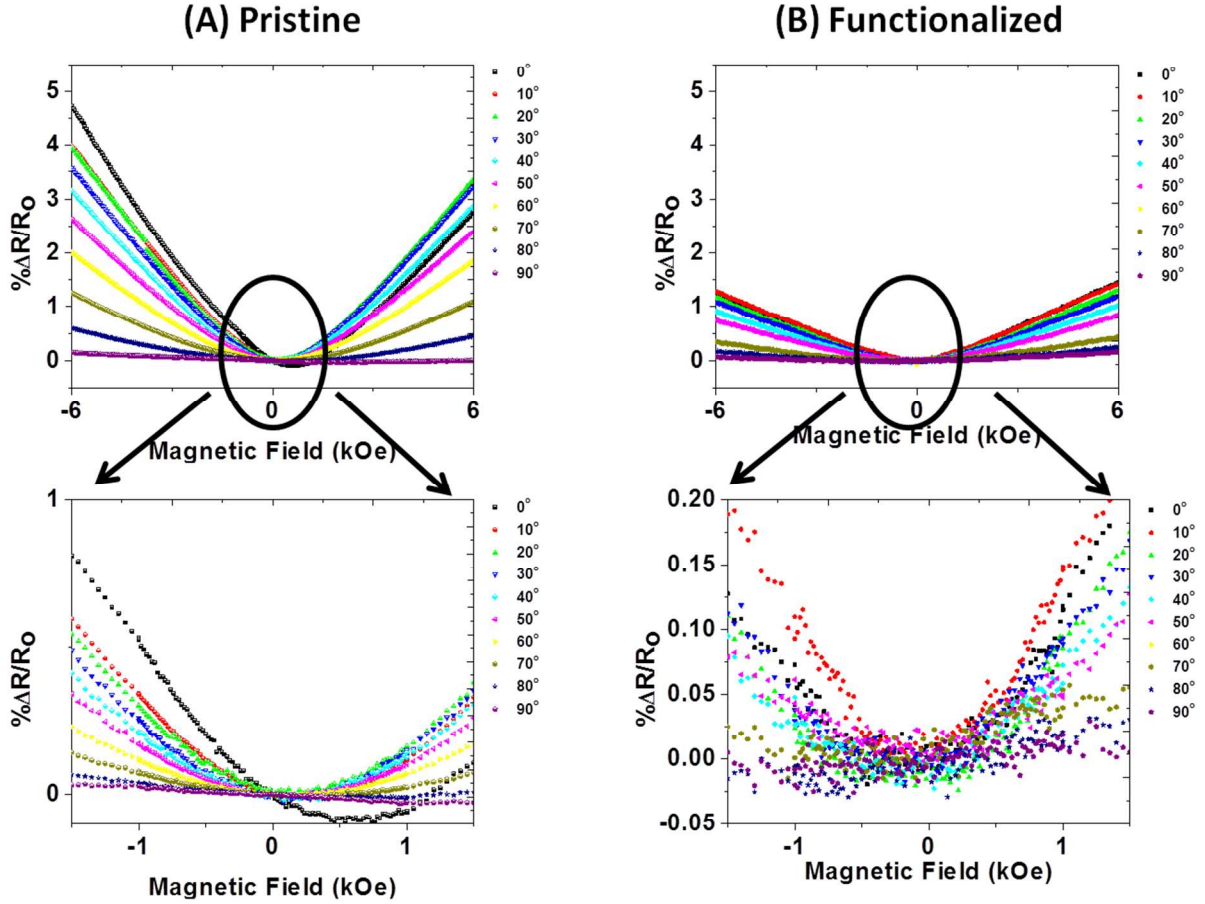


**Figure S5.** Rotation measurements of positive-MR at angles from out-of-plane to in-plane. The fit to the MR is slightly asymmetry before functionalization and symmetric after functionalization. This is a signature of non-uniformity, such as the rotational stacking default based on a change in scattering mechanism. This type of transition from asymmetry to symmetry was observed *via* EFM and Raman spectroscopy. Proper control of the positive MR in

functionalized graphene could lead the control of future magnetoelectric devices through external forces such as an electric field.

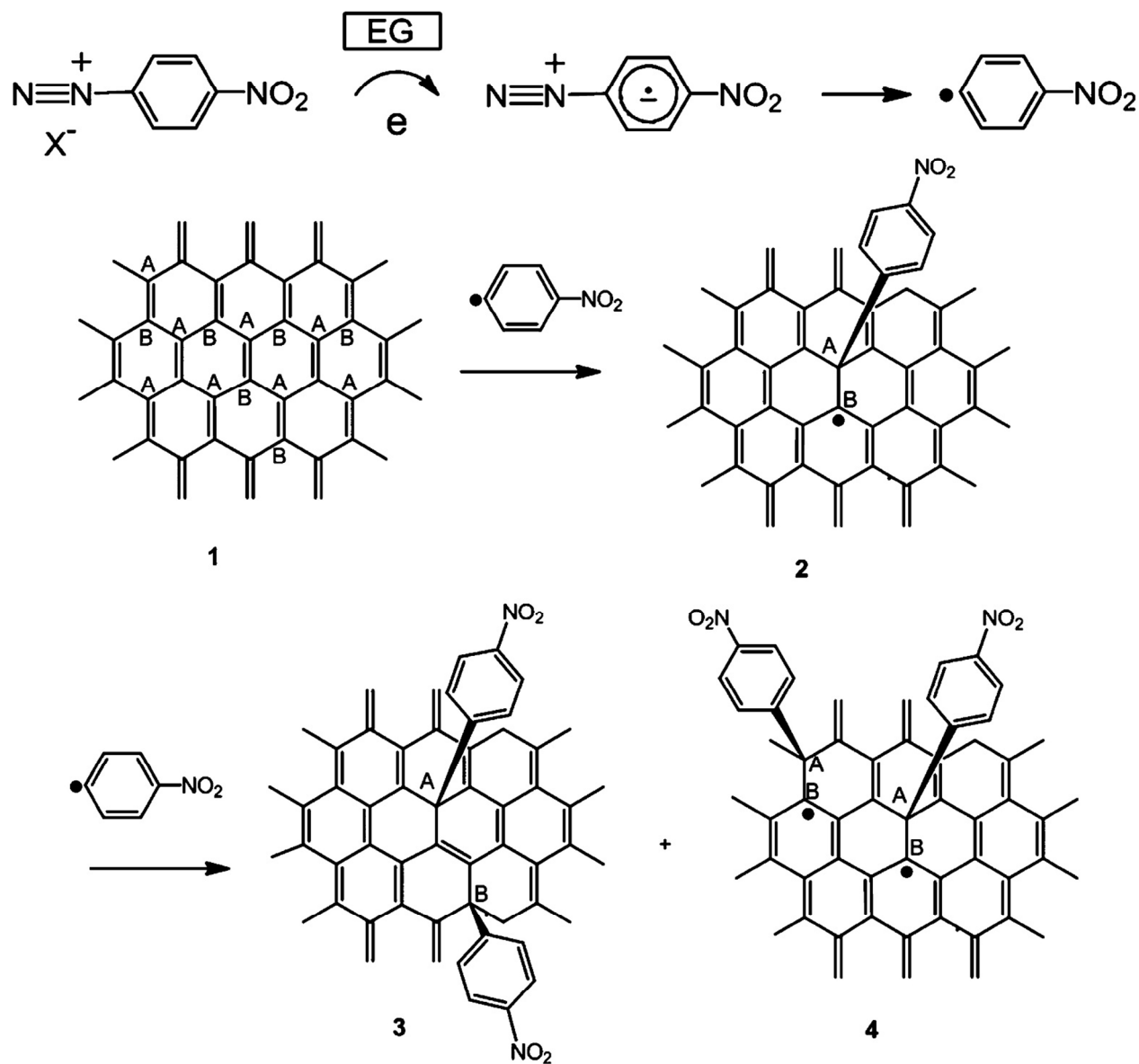


**Figure S6.** Schematic diagrams of the chemically functionalized nanoribbons: structures of the NP-functionalized epitaxial graphene products formed by spontaneous electron transfer from EG to p-nitrobenzene diazonium salt. The structure of the products 3 is expected to be antiferromagnetic whereas structure 4 would yield a ferromagnetic interaction between the spins.

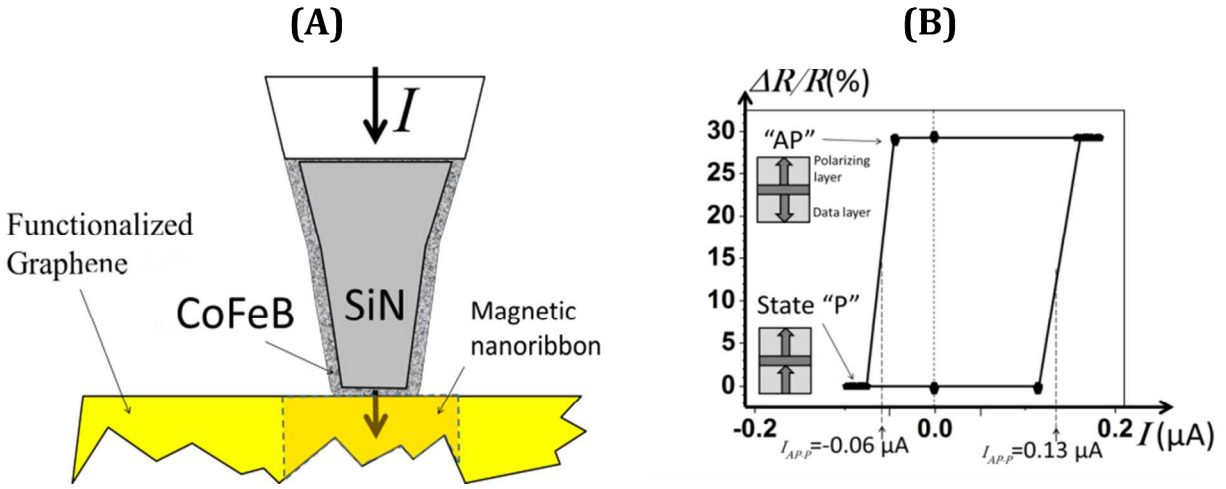


**Figure S7.** (A) A possible schematic illustration of a 3D nano-MTJ between the metal tip and a chemically isolated nanoribbon to enable STT-based energy-efficient information switching for further experiment. (B) I-R plot for Ta/CoFeB/MgO/CoFeB/Ta structures with a copper substrate. These results would be useful in applications for CINs with the advantages of a long spin relaxation time and extremely low energy under the control of an external electric field.